CrossMark
click for updates

View Article Online
View Journal

Journal of
Materials Chemistry C

Accepted Manuscript

This article can be cited before page numbers have been issued, to do this please use: J. Cui, Z. Sun, Z. Du and Y. Chao, *J. Mater. Chem. C*, 2016, DOI: 10.1039/C6TC02745H.

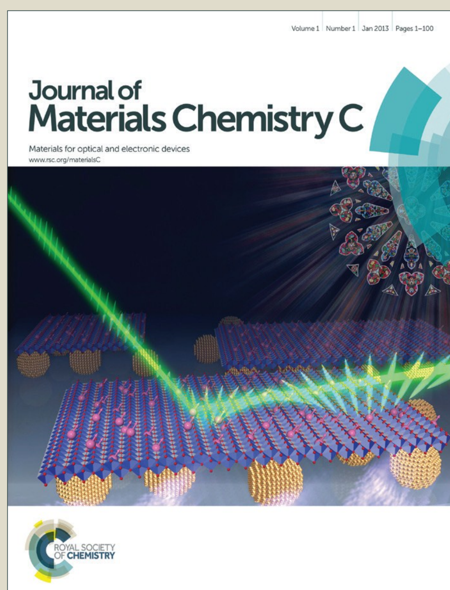

This is an *Accepted Manuscript*, which has been through the Royal Society of Chemistry peer review process and has been accepted for publication.

Accepted Manuscripts are published online shortly after acceptance, before technical editing, formatting and proof reading. Using this free service, authors can make their results available to the community, in citable form, before we publish the edited article. We will replace this *Accepted Manuscript* with the edited and formatted *Advance Article* as soon as it is available.

You can find more information about *Accepted Manuscripts* in the Information for Authors.

Please note that technical editing may introduce minor changes to the text and/or graphics, which may alter content. The journal's standard Terms & Conditions and the Ethical guidelines still apply. In no event shall the Royal Society of Chemistry be held responsible for any errors or omissions in this *Accepted Manuscript* or any consequences arising from the use of any information it contains.

ROYAL SOCIETY OF CHEMISTRY

www.rsc.org/materialsC

View Article Online
DOI: 10.1039/C6TC02745H

Journal Name

RSCPublishing

ARTICLE

Published on 04 August 2016. Downloaded by University of East Anglia Library on 09/08/2016 15:51:05.

Journal of Materials Chemistry C Accepted Manuscript

Cite this: DOI: 10.1039/x0xx00000x

Received 00th January 2016,
Accepted 00th January 2016

DOI: 10.1039/x0xx00000x

www.rsc.org/

Engineering the energy gap near the valence band edge in Mn-incorporated $Cu_3Ga_5Te_9$ for an enhanced thermoelectric performance

Jiaolin Cui[1*] , Zheng Sun[1,2], Zhengliang Du[1], Yimin Chao[3*]

$Cu_3Ga_5Te_9$ – based compounds $Cu_{3-x}Ga_5Mn_xTe_9$ (x=0-0.2) with Mn substitution for Cu have been synthesized. The engineered energy gap (ΔE_A) between impurity and valence band is reduced from 44.4 meV at x=0 to 25.7 meV at x=0.1, which is directly responsible for the reduction of potential barrier for thermal excitation of carriers and enhancement in carrier concentration. However, the Seebeck coefficient shows an increasing tendency with the increasing of determined Hall carrier concentration (n). This anomalous behavior suggests that the Pisarenko plots under assumed effective masses do not fit the current relationship between the Seebeck coefficient and carrier density. With the combination of enhanced electrical conductivities and reduced thermal conductivities at high temperatures, the maximum thermoelectric (TE) figure of merit (ZT) of 0.81 has been achieved at 804 K with x=0.1, which is about 1.65 and 2.9 times the value of current and reported intrinsic $Cu_3Ga_5Te_9$. The remarkable improvement in TE performance proves that we have succeeded in engineering the energy gap near the valence band edge upon Mn incorporation in $Cu_3Ga_5Te_9$.

1. Introduction

Thermoelectric (TE) material is capable of converting heat to electricity without using moving mechanical components or hazardous working fluids, and its TE performance is mainly evaluated by the figure of merit (ZT), $ZT=T\alpha^2\sigma/\kappa$, where T is absolute temperature, α is the Seebeck coefficient, σ is the electrical conductivity and κ is the thermal conductivity consisting of electronic (κ_e) and lattice (κ_L) components.

In addition to tellurides,[1-3] half-Heuslers[4,5] and silicides[6,7] developed as potential TE materials, the ternary chalcopyrite – structured systems based on Cu – Ga(In) – Te semiconductors have attracted much attention in recent years due to their unique crystal structures.[8−10] However, the TE performance for most of these intrinsic chalcopyrites is rather low because the decreasing rate of the Hall mobility (μ) is larger than that of the κ_L, though the presence of vacancies could reduce the Hall mobility and the lattice thermal conductivity simultaneously.[11]

Among $(Cu_2Te)_{1-y}(Ga_2Te_3)_y$ material type, $Cu_3Ga_5Te_9$ (y=0.625) (CGT) is one of the chalcopyrite – structured pseudobinary alloys with non-stoichiometric composition.[12,13] It is a potential candidate for TE materials because it possesses a relatively optimal carrier (hole) concentration n ($\sim10^{25}$ m^{-3})[12,14] at room temperature (RT). However, this compound has an ordered array of defect pairs $Ga_{Cu}^{2+}+2V_{Cu}^{-}$ (metal Ga – on – Cu antisites and two Cu vacancies), which remarkably scatters charge carriers,[15,16] leading to the reduction in mobility μ (as low as 7.70 cm^2/Vs at RT). In addition, the thermal conductivity of this material is in a region of high levels (~2.6 $WK^{-1}m^{-1}$ at RT and ~1.7 $WK^{-1}m^{-1}$ at ~740K),[12] resulting in a poor TE performance (ZT=~0.3 at 740K).[12]

Since Mn is an active element with low electronegativity (1.55), its oxidation states vary differently with chemical compounds and synthesis technologies. Therefore, it is usually used as a guest element to substitute host atoms.[17] In addition, if the chemical control over carrier density in $Cu_3Ga_5Te_9$ (CGT) can be achieved simply by element substitution, the carrier density in Mn-substituted CGT ($Cu_{3-x}Ga_5Mn_xTe_9$) can be estimated using the valence counting rule,[18] according to the chemical/crystal environment described below, presumably upon divalent Mn^{2+} occupation in the Cu^+ or Ga^{3+} sites respectively,

$$Cu_{3-x}\,V_{Cu,x}\,Mn_x\,e_x\,Ga_5Te_9 \qquad (1)$$

(upon divalent Mn^{2+} occupation in Cu^+ site)

$$Cu_{3-x}\,V_{Cu,x}\,Mn_x\,h_x\,Ga_5Te_9 \qquad (2)$$

(upon divalent Mn^{2+} occupation in Ga^{3+} site)

This journal is © The Royal Society of Chemistry 2013

View Article Online
DOI: 10.1039/C6TC02743H

where $V_{Cu,x}$ is the extra Cu vacancy from the deficiency of Cu, and e_x and h_x are the extra electrons and holes.

According to the formulas (1) and (2), an occupation of Mn^{2+} in Ga^{3+} site can enhance the hole concentration, due to the creation of an acceptor defect Mn_{Ga}^{-} (h_x). While the occupation in Cu^{+} site has no net contribution to the carrier density, because the generated extra copper vacancies $V_{Cu,x}$ from the deficiency of Cu are neutralized by the created defect Mn_{Cu}^{+} acting as a donor. However, if a high valence Mn ion (e.g. Mn^{4+}) is created in the environment of CGT, it is envisaged that there is a decreased p-type carrier concentration wherever Mn^{4+} occupies either Cu^{+} or Ga^{3+}site, although there is one-ninth intrinsic vacancy in CGT.[11]

Although such a chemical control has already been achieved in several Cu(Ag) – ternary chalcopyrites,[19,20] this control has not succeed in other materials yet. The reason is the formation of deep impurity level below / above the conduction / valence band,[21,22] which makes the Pisarenko plot[14] inconsistent with the fitting of the relationship between Seebeck coefficient and carrier density. For example, through the formation of new sub-bands near the original conduction or valence band edge the Seebeck coefficient (α) can be sharply increased via highly mismatched element substitutions,[23,24] without significant reduction of carrier concentration. Therefore, the modification of the band structures near Fermi level might be an alternative strategy to design high TE performance materials, in addition to the chemical control approach.

In the present work, a series of Cu-poor CGT with Mn substitution for Cu ($Cu_{3-x}Ga_5Mn_xTe_9$) have been synthesized, and a distinct strategy to improve the TE performance has been explored. With engineered energy gap (ΔE_A) between impurity level and valence band or formation of relatively shallow impurity level, a significantly enhanced figure of merit (ZT=0.81 @ 804 K) has therefore been achieved. This ZT value is about 2.9 times that of intrinsic CGT[12] and 0.21 higher than that in Sb-incorporated CGT.[17]

2. Experimental

A certain amount of materials Cu, Ga, Te, MnTe with the purity of 5N, according to the chemical formula of $Cu_{3-x}Ga_5Mn_xTe_9$ (x=0, 0.05, 0.1, 0.2), were loaded into four different vacuum silica tubes respectively, prior to being melted at 1323 K for 96 h, followed by a slow cooling process to RT in furnace.

The Hall coefficient (R_H) measurements at RT ~390 K were conducted on a Physical Property Measurement System (PPMS, Model-9) using a four probe configuration with a magnetic field sweeping between ±1.5 T, and were performed on rectangular samples with size 2×2×7 mm^3. The Hall mobilities (μ) and carrier concentrations (n) were subsequently calculated from the relations $\mu=R_H\sigma$ and $n=1/(eR_H)$ respectively, where e is the electron charge. The current and Hall voltage leads were fine copper wires, and the contacts were made of silver paste. The thermal diffusivities were measured using TC−1200RH at RT~810 K and the heat capacities (C_p) were estimated according to the relation $C_p = C_v+BT$ for the Cu−Ga−Te compounds, where the fitted B value is determined to be 0.015 J $mol^{-1}K^2$,[25] when the C_v approaches the Dulong–Petit limit.

Detailed experimental procedures, including the preparation of the samples, compositional (EPMA) and measurements of physical parameters (α, σ, absorption coefficients A, Raman spectra and the XPS spectra of above four elements, etc.), have been reported in literatures.[26,27]

3. Results and discussions

3.1 XRD and composition analyses

The x−ray diffraction patterns (Fig.S1) of titled powders show the peak positions from Mn-added samples are the same as those from intrinsic CGT, indicating the synthesized samples are crystallized in a single phase, in agreement with the results reported in *Ref.* [12]. Alternatively, the absence of additional peaks on the XRD patterns may indicate the formation of impurity phases that are soluble within the CGT matrix. Since $Cu_3Ga_5Te_9$ possesses chalcopyrite structure with the space group I-42d,[11] one can calculate the lattice parameters a and c from the XRD patterns, and estimate the anion displacement parameter (u) and tetragonal deformation (η),[28,29] as well as the mean cation-Te distances (R_{Cu-Te} and R_{Ga-Te}).[30,31]

The chemical compositions for intrinsic CGT and Mn-incorporated CGT (x=0.2) taken from a mapping of EPMA are shown in Table S1, where the number of Te moles is normalized to 9. The mapping pictures and line scan of $Cu_{3-x}Ga_5Mn_xTe_9$ (x=0.2) is presented in Fig.S2, and an insert in Fig.S2b is the energy dispersive x-ray spectrum. In Table S1 the relative molars of Cu, Ga, Te identified are close to those of as-prepared materials, except for a little deficiency in Mn. Such a deficiency might be due to limited instrument accuracy (~97%), which does not allow the exact amount of Mn in samples to be collected. In addition, the line scan analysis has revealed an almost homogeneous distribution of four elements in the matrix, as displayed in Fig.S2e,f.

Fig.1(a) shows the measured lattice constants, where an almost linear decreasing of the lattice constants a and c against the increasing of x value is observed. The fitting of relationship between the lattice constants and Mn content x follows Vegard's law, which suggests that Mn is incorporated into the crystal lattice in $Cu_3Ga_5Te_9$. Fig.1(b) are the u and η values. With Mn content increasing, the u value sharply increases from 0.2493 (x=0) to 0.2560 (x=0.1), and then decreases to 0.2542 (x=0.2); while the η value reduces from 1.001 (x=0) to 0.9870 (x=0.1) and then increases to 0.9914 (x=0.2). It is obvious that the deviation of u (η) values from 0.25 (1.0) at x=0.1 is much higher than others, which indicates that at x=0.1 the crystal distortion is the largest. These results can also be evidenced by the largest difference of the cation-Te distances (Δd) between R_{Cu-Te} and R_{Ga-Te}, see Fig.1(c)

3.2 XPS analysis

Journal of Materials Chemistry C Accepted Manuscript

Published on 04 August 2016. Downloaded by University of East Anglia Library on 09/08/2016 15:51:05.

This journal is © The Royal Society of Chemistry 2012

View Article Online
DOI: 10.1039/C6TC02745H

In order to understand the valence charges of the elements in the lattice of $Cu_{3-x}Ga_5Mn_xTe_9$, the oxidation states of Cu, Ga, Mn, and Te are investigated by using $Cu2p_{3/2}$, $Ga2p$, $Mn2p_{3/2}$, and $Te3d_{5/2}$ XPS spectra at x=0 and 0.2, which are shown in Fig.S3. The average binding energy (BE) values with uncertainties at ~±0.01 eV are listed in Table 1, in which the BE values of $Cu2p_{3/2}$ and $Te3d_{5/2}$ are around 932.5 ev and 572.7 eV respectively, which confirm the presence of Cu^+ and Te^{2-}.[32,33] The BE value of $Ga2p$ at x=0.1 is 1117.8 eV, which is corresponding to Ga^{3+}, about 0.3 eV higher than that at x=0. The higher BE value of $Ga2p$ upon Mn incorporation might be related to the strengthened bonding force of Ga-Te. However, the BE value of $Mn2p_{3/2}$ is unexpectedly high (642.3 eV), very close to those in MnO_2 or Mn^{4+} (642.2~642.4eV).[33-35] This indicates the existence of Mn^{4+} rather than Mn^{2+} or Mn^{3+}.

In order to have a better understanding on the occupation site of Mn^{4+} in the crystal lattice, Raman spectra from three samples (x=0.05, 0.1 and pure CGT) are shown in Fig.2, where the inset is the magnified plot. Generally, the Raman spectra of Mn-incorporated samples possess the resemblance to that of intrinsic CGT because the modes at 134.0 cm^{-1}, 74 cm^{-1} and 203.4 cm^{-1} of all the samples remain active. However, the modes at 122.7 cm^{-1} and 134.0 cm^{-1} become less pronounced with Mn content increasing, likely due to the increased lattice distortion. It is worth noting that a red-shift with Mn content increasing has been observed, which allows us to qualitatively correlate the frequency shift with the presence of internal stress/strain of the materials. In fact, the Raman shift is related to the strain/stress, where compressive (tensile) stress results in blue (red) shift. Therefore, the observed red shift in the Raman peak at 134.0 cm^{-1} indicates the presence of tensile stress, which confirms that Mn^{4+} (atomic radius 1.79 Å) prefers the Cu to Ga site, owing to larger size of Ga (1.81 Å) than that of Cu (1.57 Å). As such, the above assumed chemical environment (1) and (2) should be adjusted to the following formula,

$$Cu_{3-x}V_{Cu,x}Mn_x3e_xGa_5Te_9 \quad (3)$$

(upon Mn^{4+} occupation in Cu^+ site)

Therefore, there are two additional free electrons ($3e_x$-$V_{Cu,x}$) created per each formula unit upon Mn^{4+} occupation in Cu^+ sites.

3.3 Thermoelectric transport properties

In order to determine the effects of Mn incorporation in CGT on transport properties, we have measured Hall coefficients R_H, and then calculated the Hall carrier concentration n and mobility μ at RT~390 K (Fig.3). Fig.3(a) shows the R_H values are positive, and decrease with the temperature increasing, while the n values show an opposite trend against temperature in Fig.3(b). The n value at RT for the Mn-free CGT ($3.3\times10^{19}cm^{-3}$), which is lower than those from Ye et al. ($5.3\times10^{19}cm^{-3}$)[12] and Plirdpring ($1.5\times10^{20}cm^{-3}$),[11] enhances with both the temperature and Mn content up to at x=0.1, and then decreases with further Mn content increasing. However, in current work the n values at x=0.1 ($1.20\times10^{20}cm^{-3}$ at RT and $1.66\times10^{20}cm^{-3}$ at 390K) are about 3~4 times higher than that of intrinsic CGT. Besides, the n value for all samples enhances more rapidly before T=340K than it does after T=340K. Although the mobility (μ) bears little relevance to the temperature for the Mn-incorporated samples, it decreases rapidly with Mn content increasing until x=0.1(Fig.3c). The reduction of μ at $x\leq0.1$ is due to the reduced relaxation time τ or increased effective mass m^*, according to the relationship $\mu = e\tau / m^*$. Upon Mn incorporation, the τ value reduces owing to the additional charge carrier-ionized impurity scattering and charge carrier scattering by structural defects (formation of donor defects Mn_{Cu}^{3+} and increased vacancies V_{Cu^-}). It is worth noting that the mobility (μ) value (3.8~4.0 cm^2/vs) at x=0.2 (Fig.3c) is higher than that at x=0.1 due to low carrier density.

With Mn – incorporated CGT, Fig.4(a) shows that the Seebeck coefficients (α) are positive for all the samples, indicating p-type semiconducting behavior. Below ~600 K, the α value shows an increasing tendency with Mn content increasing until at x=0.1. However, above ~600 K it turns out to decrease dramatically with temperature increasing, due to intrinsic excitation of carriers. In Fig.4(b) the electrical conductivity (σ) remains almost the same below ~600 K, but increases in high temperature region and reaches the highest point at ~773K. Meanwhile, the lattice κ_L at 804 K reduces from 0.60 (x=0) to 0.12 $WK^{-1}m^{-1}$ (x=0.1) with Mn content increasing, and then enhances a little at x=0.2 (shown in Fig.4c). The measured thermal diffusivities (λ), density of sintered samples (d), shown in Fig.S4, decrease with temperature (Mn content) increasing. Therefore, the total κ values, which are calculated from the expression, $\kappa = d\lambda C_p$, decrease with temperature increasing, as shown in the inset in Fig.4c. However, the κ values are almost the same (~0.68 $WK^{-1}m^{-1}$) at 804 K when $x\geq0.05$, because of the variation in electronic component κ_e caused by the variation of σ with Mn content increasing. Nevertheless, the total κ values at $x\geq0.05$ are about 0.26 $WK^{-1}m^{-1}$ lower than that at x=0. Combining three physical parameters (α, σ, κ), the highest ZT value of 0.81 at 804 K when x=0.1 is obtained, which is 1.65 and 2.9 times higher than that of Mn-free CGT in current work (shown in Fig.4d), and that reported[12] respectively, and 0.21 higher than that in Sb-incorporated $Cu_3Ga_5Te_9$.[17]

The enhanced carrier concentration with Mn content could not be resulted from the chemical control over carrier density, because of the generation of extra electrons $2e_x$ ($2e_x$=$3e_x$ - $V_{Cu,x}$) from the creation of donor defect Mn_{Cu}^{3+} when Mn^{4+} prefers the Cu sites, according to the formula unit (3). Therefore, the enhancement in carrier density should be attributed to the structural alterations, such as the modification of the band structure or formation of some shallow impurity levels above the valence band maximum (VBM).

In order to explore the band structure modification upon Mn incorporation, the Pisarenko plots are shown in Fig.5, assuming m^* =0.8, 1.5 and 3.0m_e and T=320 K, 375 K and 395 K respectively. The data from Plirdpring[11] and Ye[12] are shown for comparison. We observed that the α values, at 295 K (labeled as dark square ■), 375K (red circle ●) and 390K (blue triangle ▲) respectively from the current work, show an increasing tendency with determined n value increasing (along the direction of the arrows in Fig.5), but they do not follow the Pisarenko plot, according to which the Seebeck

Published on 04 August 2016. Downloaded by University of East Anglia Library on 09/08/2016 15:51:05.

Journal of Materials Chemistry C Accepted Manuscript

View Article Online
DOI: 10.1039/C6TC02743H

Published on 04 August 2016. Downloaded by University of East Anglia Library on 09/08/2016 15:51:05.

Journal of Materials Chemistry C Accepted Manuscript

coefficient should decrease as the carrier concentration n enhances. This suggests that the previous assumed band structures might alter upon Mn incorporation, therefore, the Pisarenko plots under assumed effective mass do not well fit the relationship between the Seebeck coefficient and carrier density.

Likewise, the systematic increase of the Seebeck coefficient (α) with carrier concentration increasing could not be resulted from the energy gap (E_g) widening neither, because the measured E_g value remains almost unchanged (E_g=~0.94eV), see Fig.S5. Actually, if only we take a close look at the α values in Fig.4a, we may find that the maximum α values as well as the temperatures at which the maximum α values appear are roughly the same, regardless of the Mn content. This indicates that the E_g value could not vary much with the composition, based on the estimation using $E_g = 2e\alpha_{max}T$.

In this regard, in order to rationalize the above anomalous changes, we determine the activation energy or energy gap between impurity and valence band (ΔE_A) using first approximation at high temperatures.[21] The expression is simplified to be [15]

$$n_p(T) \approx A(T)\exp(-\frac{\Delta E_A}{\kappa_B T}) \quad (4)$$

where n_p is the hole concentration, which can be considered to be total Hall carrier concentration n, as the contribution n_p of the impurity band to the total n is considered to be negligible.[21] While $A(T)$ are expected to be slowly varying functions of T and can be considered as a constant. Under these conditions, we attain the ΔE_A values from the slope of the fitted lines in Fig.3b, which gradually decrease from 44.4 meV at x=0 to the lowest 25.7 meV at x=0.1, and then slightly increase to 26.3 meV at x=0.2. This indicates that the shallow donor or acceptor levels observed in Mn-incorporated CGT are only partially annihilated, which reduces the potential barrier for thermal excitation of carriers. Such an impact of the potential barrier on the existing charge carriers has also been demonstrated in $Ti_{0.1}Zr_{0.9}NiSn$ Half-Heusler matrix embedded full-Heusler (FH) quantum dots (QDs).[36] Because of the reduction of potential barrier, we thereby have observed the increase in carrier concentration n, while the Seebeck coefficient remains high. The reduction in n at x=0.2 might be due to the occupation of a large amount of Mn at the Cu site, which creates extra donors defects Mn_{Cu}^{3+}, thus partially neutralizing the p-type holes and increasing the μ value.

In ternary chalcopyrites there are at least two factors that govern the κ_L value on an atomic scale: an extra lattice mismatch and crystal structure distortion.[10] Normally, the lattice part κ_L should be reduced with the lattice mismatch (Mn content) increasing. However, the higher lattice part κ_L at x=0.2 than those at x=0.1 above 675 K is due to the reduced point defect scattering of phonons, which is caused by the reduction of the carrier concentration n via the creation of the donor defects Mn_{Cu}^{3+}. On the other hand, at x=0.1 there are the largest anion displacement and unit cell distortion, which are represented by the Δu=u-0.25 and $\Delta\eta$=η-1.0 (Fig.1b), coupled with the largest difference between the mean cation-Te distance ($\Delta d = R_{Cu\text{-}Te} - R_{Ga\text{-}Te}$) (Fig.1c). Therefore, it is reasonable that the κ_L at x=0.1 reaches the lowest value.[37] In addition, in Mn-incorporated CGT, the mean Cu-Te distance ($R_{Cu\text{-}Te}$) is much larger than the mean Ga-Te distance ($R_{Ga\text{-}Te}$), which is different from those in I-III-VI_2 systems, such as $AgInSe_2$ and $CuInTe_2$.[26,38]

4. Conclusions

In summary, we have synthesized the compound with Mn substitution for Cu in $Cu_3Ga_5Te_9$, and observed a reduction in energy gap between impurity and valence band (ΔE_A) at $x \leq 0.1$, which yields only partial annihilation between the shallow donor or acceptor levels, and facilitates thermal excitation of carriers as Mn content increases. The reduction in ΔE_A value has directly contributed to the enhancement of the carrier concentration n, although the Seebeck coefficient shows an increasing tendency with Mn content increasing at $x \leq 0.1$ when T < 600K. Coupled with the reduced thermal conductivities at a proper Mn content, we have obtained the maximum ZT of 0.81 at 804 K. This value is 1.65 and 2.9 times the value of current intrinsic $Cu_3Ga_5Te_9$ and that reported, and higher than that of Sb-incorporated $Cu_3Ga_5Te_9$.

 This journal is © The Royal Society of Chemistry 2012

View Article Online
DOI: 10.1039/C6TC02745H

Published on 04 August 2016. Downloaded by University of East Anglia Library on 09/08/2016 15:51:05.

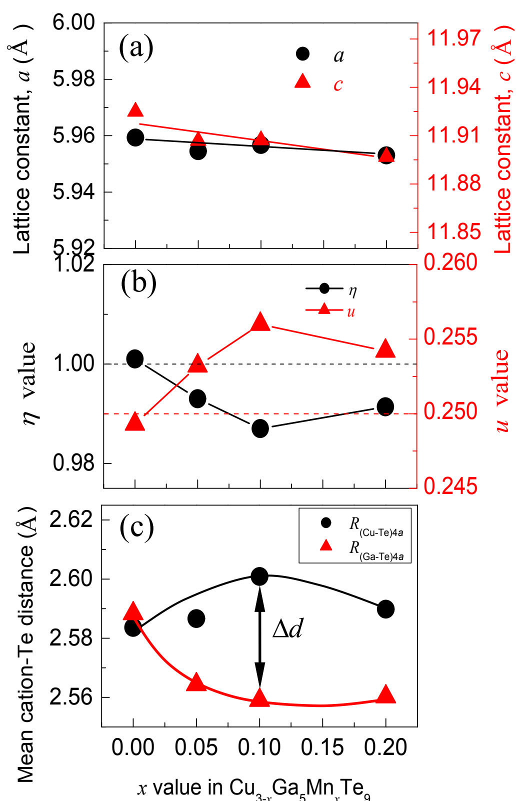

Fig.1 Mn content (x) versus lattice parameters (a, c) (a), u and η (b), and Mean cation – Te distances $R_{(Cu-Te)}$ and $R_{(Ga-Te)}$ (c), where the Δd= $R_{(Cu-Te)}$-$R_{(Ga-Te)}$, for Mn-incorporated compounds using X-ray powder diffraction experiment.

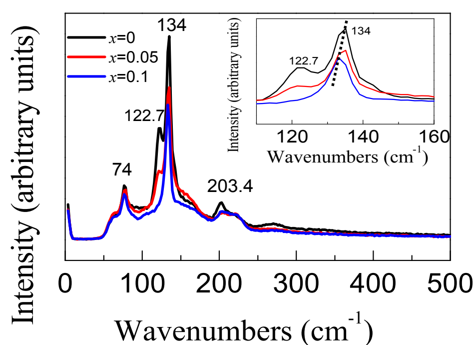

Fig.2 Raman spectra of $Cu_{3-x}Ga_5Mn_xTe_9$ (x = 0, 0.05 and 0.1) samples.

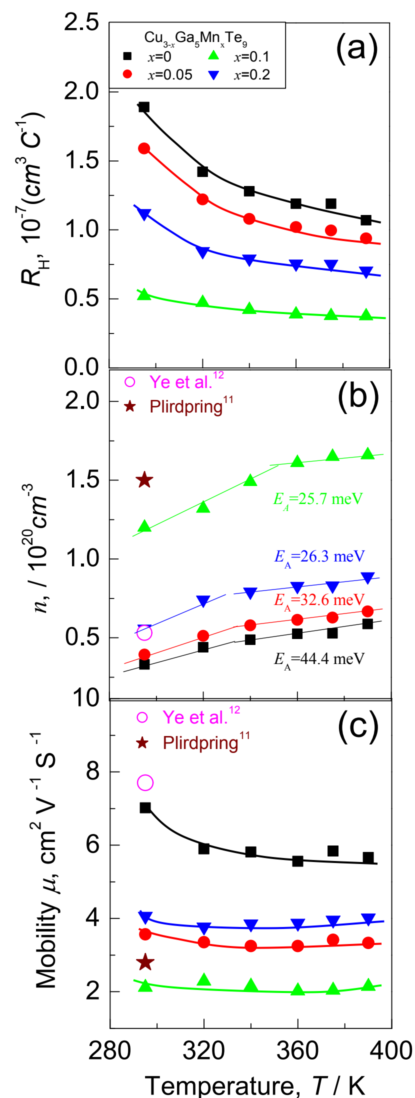

Fig.3 Hall coefficients R_H (a), Hall carrier concentration (n) (b), and mobility (μ) (c) as a function of temperature, where the n and μ values from Plirdpring[11] and Ye[12] are shown for comparison.

Journal of Materials Chemistry C Accepted Manuscript

View Article Online
DOI: 10.1039/C6TC02743H
Published on 04 August 2016. Downloaded by University of East Anglia Library on 09/08/2016 15:51:05.
Journal of Materials Chemistry C Accepted Manuscript

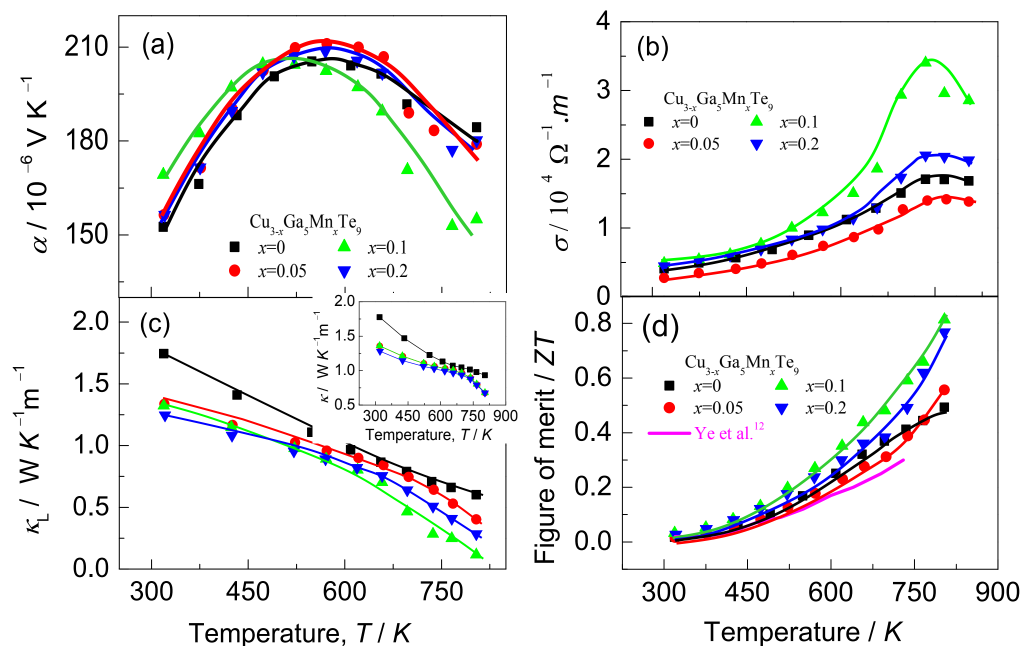

Fig. 4. Thermoelectric properties of Mn-incorporated $Cu_3Ga_5Te_9$, (a) Seebeck coefficients (α), (b) electrical conductivities (σ), (c) lattice thermal conductivities (κ_L) (an inset is the total thermal conductivity (κ), (d) *ZT* values, the data from Ye[12] is displayed for comparison.

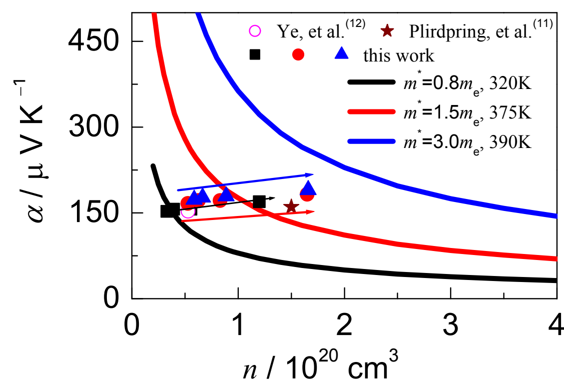

Fig.5 The Pisarenko plots assuming m^* =0.8, 1.5 and 3.0m_e and T=320 K, 375 K and 395 K respectively. The data labeled by ■, ● and ▲ represent the α values in this work at 295K, 375K and 390K with determined n_H values. The data from Plirdpring[11] and Ye[12] are shown for comparison.

Table 1 Binding energies of Mn2*p*, Cu2*p*, Ga2*p*, and Te3*d* core-level photoelectron spectra for $Cu_{3-x}Ga_5Mn_xSe_9$ (x=0, 0.2) compounds.

Compound	$Mn2p_{3/2}$ (eV)	$Cu2p_{3/2}$ (eV)	Ga2p (eV)	$Te3d_{5/2}$ (eV)
$Cu_3Ga_5Te_9$	------	932.5	1117.5	572.7
$Cu_{2.8}Ga_5Mn_{0.2}Te_9$	642.3	932.4	1117.8	572.7

This journal is © The Royal Society of Chemistry 2012

View Article Online
DOI: 10.1039/C6TC02745H

Acknowledgements

This work is supported by the National Natural Science Foundation of China (51171084), Zhejiang Provincial Natural Science Foundation (LY14E010003). We should also thank the contribution to the analyses of the experimental results by professor Shaoping Chen from Taiyuan University of Technology.

Notes and references

[1] School of Materials & Engineering, Ningbo University of Technology, Ningbo 315016, China.
[2] Materials Science and Engineering College, Taiyuan University of Technology, Taiyuan, 030024, China
[3] School of Chemistry, University of East Anglia, Norwich NR4 7TJ, United Kingdom
* Corresponding author, J.L.Cui, E-mail: cuijiaolin@163.com; E-mail:Y.Chao@uea.ac.uk

Electronic Supplementary Information (ESI) available: XRD patterns, EPMA mapping, chemical composition and .the absorption coefficients analyses, See DOI: 10.1039/b000000x/

Published on 04 August 2016. Downloaded by University of East Anglia Library on 09/08/2016 15:51:05.

Journal of Materials Chemistry C Accepted Manuscript

View Article Online
DOI: 10.1039/C6TC02743H

Published on 04 August 2016. Downloaded by University of East Anglia Library on 09/08/2016 15:51:05.

Journal of Materials Chemistry C Accepted Manuscript

REFERENCES

1 Y.Pei, X.Shi, A.LaLonde, H.Wang, L.Chen and G.J.Snyder, *Nature*, 2011,**473**,66.

2 Y.Gelbstein, Z. Dashevsky and M.P. Dariel, *Physica B*, 2007, **396**, 16.

3 J. Davidow and Y. Gelbstein, *J. Electron. Mater.*, 2013, **42**, 1542.

4 K. Kirievsky, Y. Gelbstein and D. Fuks, *J. Solid State Chem.*, 2013, **203**, 247.

5 Y.Gelbstein, N. Tal, A. Yarmek, Y. Rosenberg, M.P. Dariel, S. Ouardi, B. Balke, C. Felser and M. Köhne, *J. Mater. Res.*, 2011, **26**, 1919.

6 W.Liu, X.J.Tan, K.Yin, H.J.Liu, X.F.Tang, J.Shi, Q.J.Zhang and C.Uher, *Phys. Rev. Lett.*, 2012,**108**,166601.

7 Y. Sadia, L. Dinnerman and Y. Gelbstein, *J. Electron. Mater.*, 2013, **42**,1926.

8 T.Plirdpring, K.Kurosaki, A.Kosuga, T.Day, S.Firdosy, V.Ravi, G.J.Snyder, A. Harnwunggmoung, S T.ugahara, Y.Ohishi, H.Muta and S.Yamanaka, *Adv. Mater.*, 2012, **24**, 3622.

9 J.Zhang, R.Liu, N.Cheng, Y.Zhang, J.Yang, C.Uher, X.Shi, L.Chen and W.Zhang, *Adv. Mater.*, 2014,**26**, 3848.

10 J.Cui, Y.Li, Z.Du, Q.Meng and H.Zhou, *J. Mater.Chem.* A, 2013, **1**, 677.

11 T.Plirdpring, K.Kurosaki, A.Kosuga, M.Ishimaru, A.Harnwunggmoung, T.Sugahara, Y.Ohishi, H.Muta and S.Yamanaka, *Mater. Trans.*, 2012, **53**, 1212.

12 Z.Ye, J.Cho, M.M.Tessema, J.R.Salvador, R.A.Waldo, H.Wang and W.Cai, *J. Solid State Chem.*, 2013, **201**, 262.

13 C.Julien, I.Ivanov, A.Khelfa, F.Alapini and M.Guittard, *J. Mater. Sci.*, 1996, **31**, 3315.

14 G.J.Snyder and T E.S.oberer, *Nat. Mater.*, 2008, **7**, 105.

15 C.Rincón, S.M.Wasim and G.Marín, *Appl. Phys. Lett.*, 2002, **80**, 998.

16 C.Rincón, S.M.Wasim, G.Marín, J.M.Delgado and J.Contreras, *Appl.Phys.Lett.*, 2003,**83**, 1328.

17 Z.Sun, S.Chen, J.Yang, Q.Meng and J.Cui, *Acta Phys. Sin.* (in Chinese), 2014, **63**, 057201.

18 E.S.Toberer, A.F.May and G.J.Snyder, *Chem. Mater.*, 2010, **22**, 624.

19 A.Yusufu, K.Kurosaki, A.Kosuga, T.Sugahara, Y.Ohishi, H.Muta and S.Yamanaka, *Appl.Phys.Lett.*,2011, **99**, 061902.

20 A.Kosuga, T.Plirdpring, R.Higashine, M.Matsuzawa, K.Kurosaki and S.Yamanaka, *Appl.Phys.Lett.* 2012, **100**, 042108.

21 L.Essaleh, S.M.Wasim and J.Galibert, *J. Appl. Phys.*, 2001, **90**, 3993.

22 L.Lin, J. H.Wernick, N.Tabatabaie, G,W.Hull and B.Meagher, *Appl.Phys.Lett.*, 1987, **51**, 2051.

23 W.Shan, W.Walukiewicz, J.W.Ager III, K.M.Yu and J.Wu, *Appl. Phys. Lett.*, 2003, **83**, 299.

24 J.Lee, J.Wu and J.C.Grossman, *Phys. Rev. Lett.*, 2010, **104**, 016602.

25 D.F.Zou, S.H.Xie, Y.Y.Liu, J.Lin and J.Li, *J. Alloys Compds.*, 2013, **570**, 150.

26 J.Cui, L.Wang, Z.Du, P.Ying and Y.Deng, *J. Mater. Chem. C*, 2015,**3**, 9069.

27 M.Cheng, S.Chen, Z.Du, X.Liu and J.Cui, *Phys. Status Solidi A*, 2016, DOI 10.1002/pssa.201600003

28 S.C.Abrahams and J.L.Bernstein, *J.Chem.Phys.*,1973,**59**, 5415.

29 S.C.Abrahams and J.L.Bernstein, *J. Chem. Phys.*, 1974, **61**, 1140.

30 J.E.Jaffe and A.Zunger, *Phys. Rev. B.*, 1984, **29**,1882.

31 J.E.Jaffe and A.Zunger, *Phys. Rev. B.*, 1983, **28**,5822.

 This journal is © The Royal Society of Chemistry 2012

View Article Online
DOI: 10.1039/C6TC02745H

32 S.Chen, W.Ren, Q.Meng, X.Liu, J.Yang and J.Cui, *Phys. Status Solidi A*, 2014, **211**, 618.

33 J.F.Moulder and J.Chastain, *Handbook of X-ray Photoelectron Spectroscopy: A Reference Book of Standard Spectra for Identification and Interpretation of XPS Data*, Perkin–Elmer Corporation, Physical Electronics Division: Eden Prairie, Minnesota, 1992, p. 261.

34 R.J.Iwanowski, M.H.Heinonen and E.Janik, *Chem. Phys. Lett.*, 2004, **387**, 110.

35 B.Murugan and A.V.Ramaswamy, *J. Phys. Chem. C*, 2008, **112**, 20429.

36 Y.G.Liu, P.Sahoo, J.P.A.Makongo, X.Zhou, S.Kim, H.Chi, C.Uher, X.Pan, P.F.P.Poudeu, *J.Am.Chem. Soc.*, 2013, **135**, 7486.

37 W.Wu, Y.P.Li, Z.L.Du, Q.S.Meng, Z.Sun, W.Ren and J.Cui, *Appl.Phys.Lett.*, 2013, **103**, 011905.

38 J.Yang, S.Chen, Z.Du, X.Liu and J.Cui, *Dalton Trans.*, 2014, **43**, 15228.

Published on 04 August 2016. Downloaded by University of East Anglia Library on 09/08/2016 15:51:05.

Journal of Materials Chemistry C Accepted Manuscript

This journal is © The Royal Society of Chemistry 2012

View Article Online
DOI: 10.1039/C6TC02745H

Published on 04 August 2016. Downloaded by University of East Anglia Library on 09/08/2016 15:51:05.

Table of Contents (TOC)

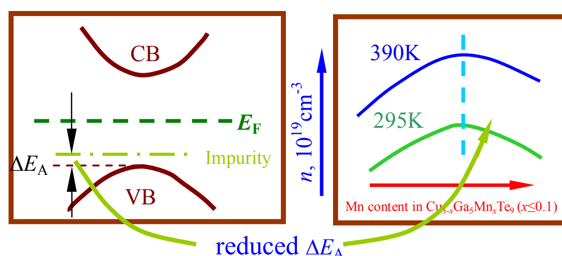

Mn substitution for Cu in $Cu_3Ga_5Te_9$ engineers the energy gap (ΔE_A) between impurity and valence band, which is responsible for the reduction of potential barrier for thermal excitation of carriers.

Journal of Materials Chemistry C Accepted Manuscript

View Article Online
DOI: 10.1039/C6TC02745H
Published on 04 August 2016. Downloaded by University of East Anglia Library on 09/08/2016 15:51:05.
Journal of Materials Chemistry C Accepted Manuscript